Preprint
UCRL-JC-147710

Investigation of the Kinetics of the Ferrite/Austenite Phase Transformation in the HAZ of a 2205 Duplex Stainless Steel Weldment

T. A. Palmer, J. W. Elmer, J. Wong, S. S. Babu, J. M. Vitek

U.S. Department of Energy
Lawrence Livermore National Laboratory

This article was submitted to
6th International Conference on Trends in Welding Research, Pine Mountain, GA., April 15-19, 2002

March 14, 2002

This work was performed under the auspices of the United States Department of Energy by the University of California, Lawrence Livermore National Laboratory under contract No. W-7405-Eng-48.

Investigation of the Kinetics of the Ferrite/Austenite Phase Transformation in the HAZ of a 2205 Duplex Stainless Steel Weldment

T.A. Palmer, J.W. Elmer, and Joe Wong
Lawrence Livermore National Laboratory
Livermore, CA 94550

S.S. Babu and J.M. Vitek
Oak Ridge National Laboratory
Oak Ridge, TN 37831

A semi-quantitative map based on a series of spatially resolved X-ray diffraction (SRXRD) scans shows the progression of the ferrite (δ)/austenite (γ) phase balance throughout the HAZ during GTA welding of a 2205 duplex stainless steel (DSS). This map shows an unexpected decrease in the ferrite fraction on heating, followed by a recovery to the original ferrite fraction on cooling at locations within the HAZ. Even though such behavior is supported by thermodynamic calculations, it has not been confirmed by either experimental methods or have the kinetics been evaluated. Both Gleeble thermal simulations and time resolved x-ray diffraction measurements on spot welds in the 2205 DSS provide further evidence for this rather low-temperature transformation. On the other hand, calculations of the diffusion of alloying elements across the δ/γ interface under a variety of conditions shed no further light on the driving force for this transformation. Further work on the mechanisms and driving forces for this transformation is on-going.

Introduction

Spatially resolved x-ray diffraction (SRXRD) is a unique technique for the real time *in-situ* monitoring of phase transformations occurring during the heating and cooling cycles typical of welding. A number of materials systems have been studied using this technique, ranging from commercially pure titanium, to AISI 1005 plain carbon steels to flux core arc welding electrode materials.[1-8]

Recent SRXRD measurements have been made on 2205 duplex stainless steel (DSS) GTA welds.[9] The 2205 DSS material studied here is characterized by a duplex structure of nearly equal amounts of ferrite (bcc) and austenite (fcc). This material has been studied because it provides the opportunity to monitor how this duplex structure evolves under the conditions prevalent in the HAZ of a weld.

The δ/γ phase balance in the HAZ evolves during the heating and cooling cycles of the welding process. This phase balance at a specific location can be semi-quantitatively determined by measuring the areas of the individual ferrite and austenite peaks in each SRXRD pattern. The peak areas measured in each SRXRD pattern are converted into the intensity fractions of austenite and ferrite, which are defined as the ratio of the sum of the measured peak area for each phase to the total peak area in a single SRXRD pattern. The technique used to convert the intensity fractions to the volume fractions of each phase is summarized elsewhere.[9]

A refined phase map, compiling all of the measurements made around the weld pool is shown in Figure 1(a). This map tracks the progress of the δ/γ phase transformation during the welding process. The temperature isotherms are calculated using a mathematical model based on turbulent heat transfer and fluid flow.[10-13] Examination of this map shows that the δ volume fraction first decreases to levels below those found in the base metal on the leading edge of the weld pool. At locations behind the weld pool, the δ volume fraction rapidly recovers to that observed in the base metal.

In order to provide an explanation for this behavior, the thermal history and δ volume fraction are plotted as a function of location along a path parallel (y=9.5 mm) to the welding direction in Figure 1(b). During heating, the δ volume fraction decreases until a minimum value is reached near the peak temperature (~750°C). As the metal starts to cool, the δ volume fraction increases rather rapidly and approaches that observed in the base metal. These observations indicate that the δ→γ phase transformation is favored during heating, up to temperatures approaching 750°C. Previous researchers have noted the possibility of the occurrence of the δ→γ phase transformation in the HAZ only during the cooling cycle.[14,15]

Thermodynamic calculations support the δ→γ phase transformation on heating. Figure 2(a&b) show plots of the thermodynamic calculations of the stability of ferrite and austenite under both equilibrium and non-equilibrium conditions. The equilibrium calculations in Figure 2(a) take into account the partitioning of the alloying elements between the two phases. On the other hand, the non-equilibrium calculations in Figure 2(b) do

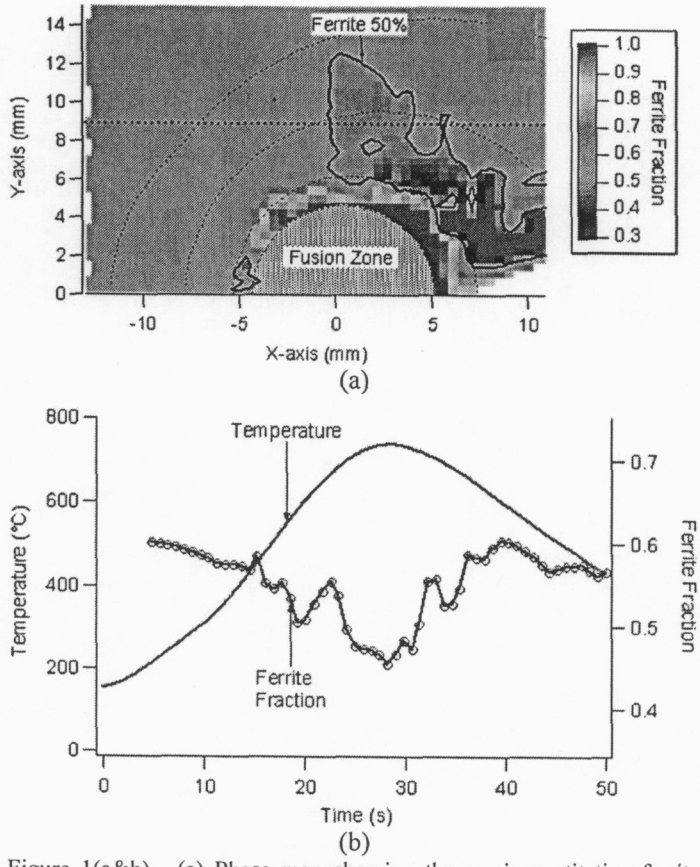

Figure 1(a&b). (a) Phase map showing the semi-quantitative ferrite volume fractions measured during SRXRD experiments. (b) Plot showing the calculated temperature profile and the ferrite volume fraction at locations 9 mm from the weld centerline.

not take into account the partitioning of the alloying elements between the phases. In both cases, though, the $\delta \rightarrow \gamma$ and the $\gamma \rightarrow \delta$ transformations are shown to be feasible during both weld heating and cooling.

While these thermodynamic calculations provide insight into the stability of δ and γ, they do not provide information about the kinetics of the $\delta \rightarrow \gamma \rightarrow \delta$ transformation on heating and cooling during welding. The objective of this work is, therefore, two-fold. First, there is a need to experimentally confirm the behavior observed in the previous SRXRD experiments. This confirmation can be made through the use of Gleeble thermal simulations and time resolved x-ray diffraction (TRXRD) of spot welds. Second, the mechanism by which this transformation occurs needs to be considered. There are a number of models available to analyze the $\delta \rightarrow \gamma$ transformation. In this case, the equilibrium and paraequilibrium diffusion of alloying elements across the δ/γ interface is considered under both isothermal and non-isothermal conditions. The combination of experimental and modeling studies performed here should provide the basis for determining the transformation mechanism.

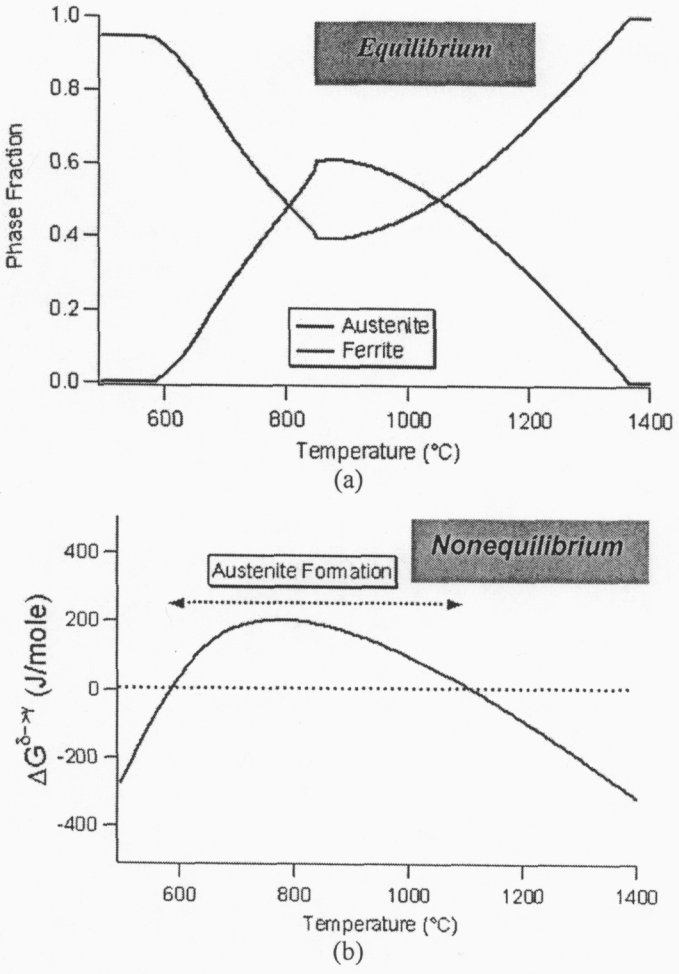

Figure 2(a&b). Plots showing the stability of ferrite and austenite under both (a) equilibrium and (b) non-equilibrium conditions over the temperature range where the $\delta \rightarrow \gamma \rightarrow \delta$ transformation is observed.

Experimental

Gleeble Thermal Simulations

A series of thermal simulations, similar to those calculated to occur within the HAZ during the GTA welding of the 2205 DSS (22.43 Cr-4.88 Ni-3.13 Mo-1.40 Mn-0.023 C-0.18 N-0.004 S-0.005 O-0.0007H-0.67 Si-0.02 Al-0.03 B-0.08 Co-0.20 Cu-0.03 Nb-0.028 P->0.005 Ti-0.05 V- Bal. Fe) described above, have been performed on a Gleeble® 3500 Thermomechanical Simulator. Rods, approximately 6.35 mm in diameter have been machined from as-received forged bar. The as-received material has been solution annealed at 1065°C for 2.5 hours followed by water quenching to ambient temperatures. This forged bar is the same material from which the SRXRD and TRXRD sample bars have been fabricated.

High resolution radial dilatometry is used to measure the strain produced during the programmed thermal cycles. These heat treatments simulate the typical heating and cooling cycles experienced in the regions of the weld HAZ where the $\delta \rightarrow \gamma \rightarrow \delta$ transformation is observed. In particular, the sample is heated to 740°C at a rate of approximately 30°C/sec, undergoes a 4 sec. isothermal hold at this temperature in order to equilibrate the

sample before cooling to room temperature at a rate of approximately 15°C/sec. In order to test the response of the system, a pure nickel calibration sample has been tested under the simulated weld HAZ thermal cycle. No evidence for a phase transformation, such as a change in the slope of the temperature strain curve, over both heating and cooling is observed.

TRXRD Experiments

The TRXRD experiments are performed on the 31-pole wiggler beam line (BL 10-2)[16] at the Stanford Synchrotron Radiation Laboratory (SSRL) on the Stanford Positron-Electron Asymmetric Ring (SPEAR). In this setup, the synchrotron beam emerges from the wiggler and is focused by a toroidal mirror to a size of approximately 1 mm high x 2 mm wide and monochromatized with a double Si(111) crystal. The focused beam then passes through a 540 μm tungsten pinhole to render a submillimeter beam on the sample at an incident angle of approximately 25°. These portions of the experimental set-up are shown schematically in Figure 3.

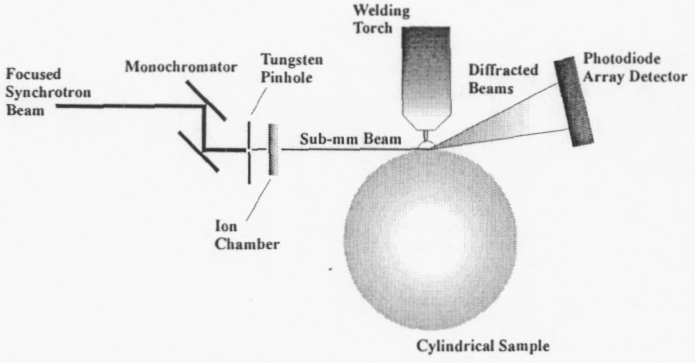

Figure 3. Schematic diagram of the TRXRD experimental set-up.

A photon energy of 12.0 keV (λ = 0.1033 nm) has been chosen to maximize the number of observable diffraction peaks and to ensure that the photon energy is high enough above the Fe K-edge (7.112 keV) and the Ni K-edge (8.332 keV) to minimize the K-fluorescence contribution from the sample. Within the 2θ range examined here (approximately 25° to 57°), there are three peaks associated with the bcc (δ-Fe) and four peaks associated with the fcc (γ-Fe) phases in the 2205 DSS.[17] Further details regarding the experimental set-up are described in detail elsewhere.[1-8]

Unlike the SRXRD experiments described previously, the bar is not rotated beneath the fixed electrode here. In this case, a spot weld is made on the bar, and the x-ray is kept at a position a fixed distance from the welding electrode and, in turn, the fusion zone boundary. During the spot welding process, 600 measurements are taken at 50 to 200 msec intervals, allowing the transformations to be tracked as a function of time.

These GTA spot welds are made using a peak current of 130 A and a background current of 90 A, pulsed at a frequency of 300 Hz. The pulsing parameters are designed to minimize the side-to-side motion of the liquid weld pool, thus decreasing the potential experimental error in the location of the liquid/solid interface. The arc gap is set at a distance of 0.28 cm, correlating to an arc voltage of approximately 17 V, and welding was performed using a W-2% Th electrode with a diameter of 0.47 cm. Shielding is provided to the weld pool by high-purity (99.999%) helium being flowed through the torch and from a helium side blow, which removes soot (condensed metal vapors) from the area being examined with the synchrotron x-rays.

To avoid contamination of the weld metal with the external atmosphere, welding is performed in an environmentally sealed chamber. The welding process is monitored with an infrared (IR) camera (FLIR, Inc. Model SC1000). Prior to welding, the chamber is evacuated to a vacuum level of approximately 8 Pa using a mechanical roughing pump, after which the chamber is backfilled with helium until it reaches atmospheric pressure.

Results and Discussion

Gleeble Thermal Simulations

Figure 4 shows a plot of the measured diametrical strain in a 2205 DSS rod during a simulated weld HAZ thermal cycle. There are several interesting features to this figure. During the heating cycle, there is a visible change in the slope of the strain/temperature curve, which is expected to be linear, at a temperature between approximately 400°C and 450°C. This change in slope indicates that there is potentially a phase transformation occurring in this temperature range. A phase transformation at these temperatures corresponds to what is observed in the SRXRD experiments. Upon cooling, there is also a significant change in the diametrical strain, starting at temperatures of approximately 650°C. As the cooling cycle continues, the sample continues to contract, and the cycle ends with no measured plastic strain in the sample.

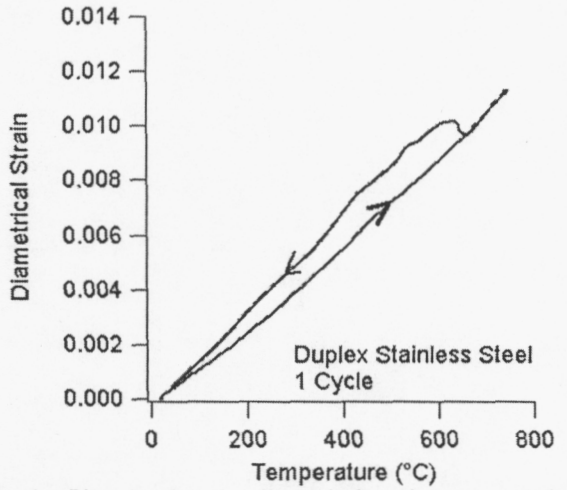

Figure 4. Plot showing the diametrical strain measured during the simulated weld thermal cycle.

Since the sample exhibits no plastic strain after a single thermal cycle, the effects of multiple thermal cycles are investigated. Figure 5 shows the diametrical strain as a function of temperature for two thermal cycles run consecutively on the same sample. There is little to no difference in the behavior of the sample in each run, and the sample shows the same strain/phase transformation behavior as that in Figure 4. This behavior indicates that there is the potential for a reversibility of

this transformation. Further work is required to better understand this behavior.

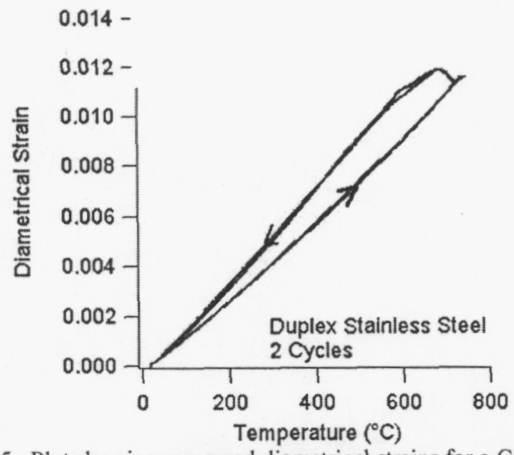

Figure 5. Plot showing measured diametrical strains for a Gleeble sample exposed to consecutive simulated weld HAZ thermal cycles.

The measured diametrical strains in the samples can be further evaluated by the application of a geometric model to determine the ferrite fraction present in the sample at each temperature in the thermal cycle. This technique is based upon a previously published geometric model[18] and takes advantage of the duplex nature of the samples studied here.

In this model, temperature invariant thermal expansion coefficients are assumed for pure ferrite and austenite, as shown in Figure 6. With the theoretical curves for austenite and ferrite superimposed over the experimental curve, the fraction of each phase can be determined based on a lever rule type relationship. For example, the ferrite fraction at any given point is based on the ratio of the distance from the experimental curve to the austenite curve and the overall distance between the theoretical ferrite and austenite curves. When repeated over the heating and cooling curves, the change in ferrite fraction over the entire thermal cycle can be determined.

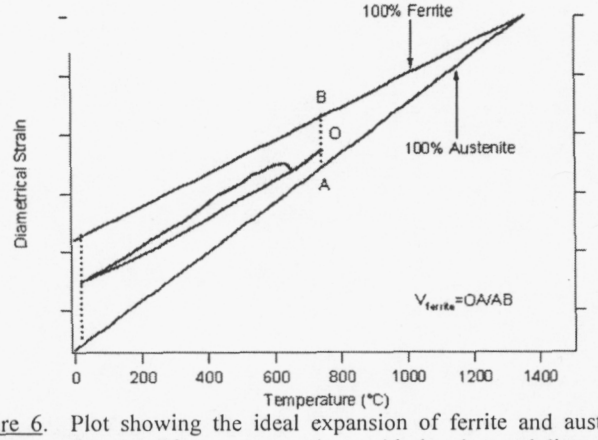

Figure 6. Plot showing the ideal expansion of ferrite and austenite phases as a function of temperature along with the observed diametrical strain behavior of the 2205 DSS.

The application of this model to the experimental strain/temperature relationships is shown in Figure 7(a) for a single thermal cycle and in Figure 7(b) for multiple thermal cycles. In each case, the ferrite fractions determined from the dilatometry experiments follow much the same trend as the previous SRXRD results. With heating, the ferrite fraction decreases rather slowly, indicating sluggish austenite growth. The onset of the cooling cycle, though, results in a rapid increase in the ferrite fraction, corresponding to a rapid transformation to ferrite in the microstructure.

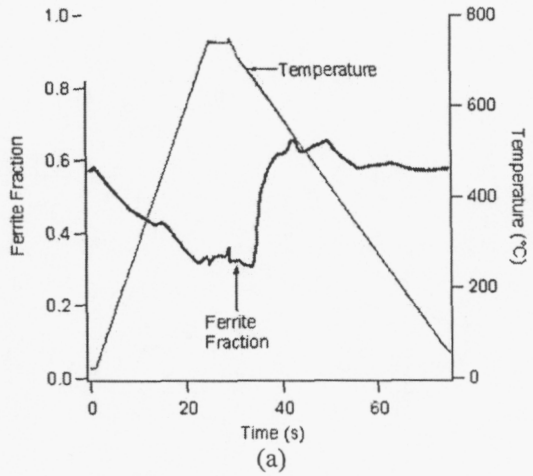

(a)

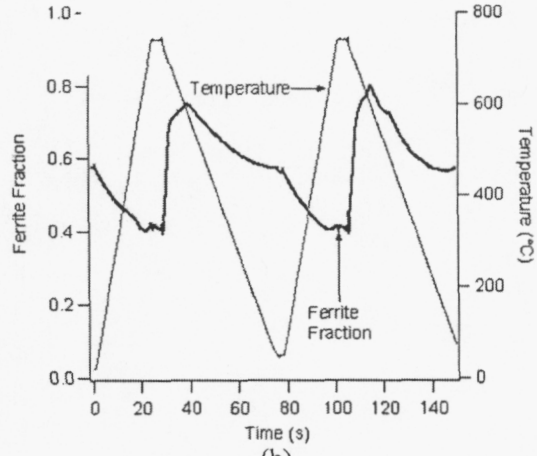

(b)

Figure 7(a&b). Plots showing ferrite volume fractions extracted from the diametric strain measurements for (a) a single thermal cycle and (b) multiple thermal cycles.

Time Resolved X-Ray Diffraction Measurements

In addition to the Gleeble thermal simulations discussed above, the change in ferrite volume fraction during the weld HAZ thermal cycle can be monitored using TRXRD techniques. These experiments allow for the change in the ferrite volume fraction at a given location to be monitored as a function of time. Figure 8(a) shows the variation in peak intensities for x-ray diffraction measurements made at a location 3 mm from the fusion zone boundary with exposure times of 200 msec. In general, there are no phase changes observed in the diffraction patterns, since both the ferrite and austenite peaks are present throughout.

On the other hand, an analysis of the peak areas to determine the ferrite volume fraction at each time shows several very interesting features of this data. Figure 8(b) shows how the ferrite volume fraction changes as a function of time during both the heating and cooling cycles experienced at this location.

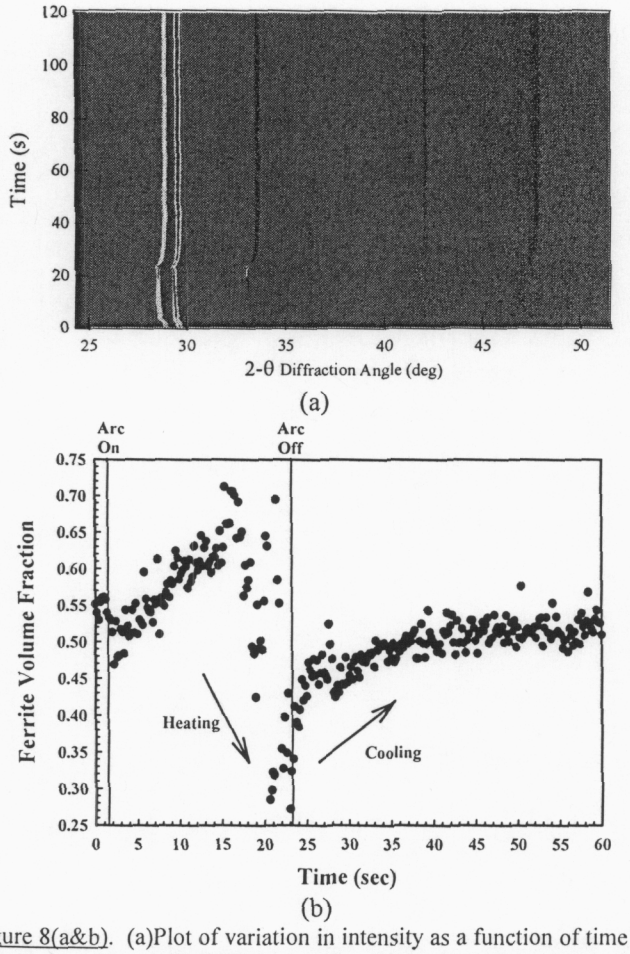

Figure 8(a&b). (a)Plot of variation in intensity as a function of time for observed peaks in a TRXRD experiment taken at a location 3 mm from the fusion line. (b) Plot of semi-quantitative ferrite volume fractions as a function of time based on measurements of the peak areas.

Similar to the trends observed during the SRXRD experiments, the ferrite volume fraction decreases during heating and subsequently increases to the base metal value during cooling. Unlike the SRXRD and Gleeble thermal simulations, no data currently exist for the thermal cycle accompanying this observed change in the ferrite volume fraction. Work is, therefore, continuing on better understanding the characteristics of this phase transformation and the thermal cycles present at these locations during spot welding.

Initial Modeling Efforts

In order to better understand the δ/γ phase transformation at these temperatures, calculations have been performed to evaluate the kinetics of the transformation. These calculations have been focused on the diffusion of both substitutional (Cr and Ni) and interstitial (C and N) elements across the interface between ferrite and austenite under equilibrium and paraequilibrium conditions. The general characteristics of the interface used in these models are shown in Figure 9(a), where the concentration of Cr and Ni in both the ferrite and austenite and the interface between the two phases is plotted. The partitioning of the alloying elements is based on electron microprobe measurements made in the base metal, and shown in Figure 9(b). Both isothermal conditions and non-isothermal conditions, simulating the thermal cycles experienced in the weld HAZ, have been considered.

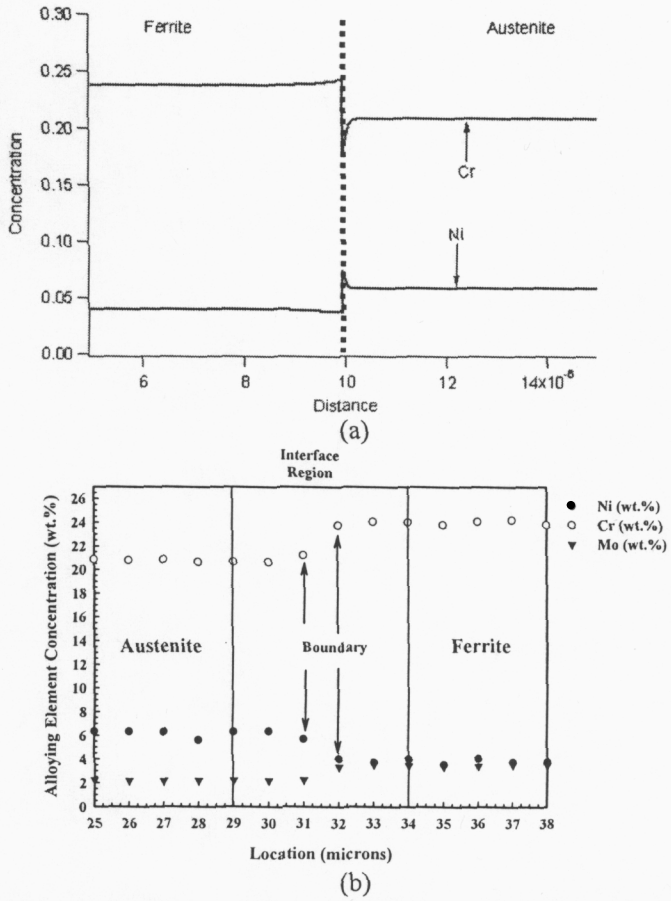

Figure 9. Plots showing (a) the concentration gradients of Cr and Ni at the boundary between ferrite and austenite used in the modeling of the phase transformation and (b) the measured concentrations of Cr, Ni, and Mo in the as-received base metal.

The results of these modeling efforts do not currently provide much evidence for the mechanisms controlling this phase transformation. In the first set of modeling calculations, the isothermal δ→γ transformation is examined using a finite difference method[19] to solve for the diffusion of Cr and Ni in both the δ and γ phases and matching the mass balance at the interface. These calculations show that in the Fe-Cr-Ni system, that the isothermal transformation at 740°C will take over 700 days to see similar transformations as those observed in welding. In fact, the isothermal transformation kinetic calculations in the Fe-Cr-Ni system show that only at temperatures above 1100°C is there any significant transformation within a time scale similar to welding. When C and N are considered in the calculations, there is again little movement of the interface. The integration of thermal cycles typical of the welding condition also produce little change. These results indicate that the observed transformations cannot be explained by diffusion controlled growth with local equilibrium at the δ/γ interface.

Calculations assuming paraequilibrium nitrogen diffusion across the interface have also been attempted.[20] In these calculations, the substitutional elements (Fe, Cr, and Ni) are configura-

tionally frozen during the transformation, and only the diffusion of nitrogen controls the transformation. The calculations show, though, the kinetics of the reaction to be reversed. Specifically, the reverse transformation is sluggish during cooling, while the heating transformation is rapid. Much is not known of the mechanisms for this type of transformation in this alloy, and work is continuing.

Another mechanism for this observed phase transformation is also receiving attention here. In previous work,[21-22] it is shown that localized stresses can develop between the δ/γ interface due to differences in the thermal expansion coefficient of the two phases. If the stresses are high enough, it is possible to sustain a displacive transformation to relieve the stresses. Further work is required in this area.

Summary and Conclusions

Both Gleeble thermal simulations and TRXRD experiments on the 2205 DSS material of interest have been performed. Each set of experiments provides confirming evidence for the low temperature δ→γ transformation first observed in the SRXRD results.

Gleeble Thermal Simulations:

A. Dilatometric strains are observed at the same temperatures within the heating and cooling cycles as where the changes in the ferrite volume fraction are observed in the SRXRD experiments.

B. Geometric conversion of the strains to the corresponding ferrite volume fractions demonstrate similar behavior to the SRXRD experiments.

C. The δ→γ→δ transformation on heating and cooling appears to be reversible, even after numerous thermal cycles.

TRXRD Experiments

D. TRXRD experiments allow the δ→γ→δ transformation during both the welding heating and cooling cycles to be monitored as a function of time.

E. A semi-quantitative analysis of the ferrite volume fractions at each point in time during the TRXRD analysis of a 2205 DSS spot weld shows similar behavior to that observed in the previous SRXRD experiments.

Initial Modeling Results

F. Modeling of diffusion controlled growth involving C, N, Cr, and Ni does not appear to be the mechanism for this reaction.

G. Paraequilibrium diffusion controlled growth involving interstitial diffusion is possible, but the rates of the transformations on heating and cooling are the reverse of those observed.

H. The potential for a deformation induced transformation is addressed and requires further study.

The work reported here represents a preliminary study of this low temperature phase transformation. Further work is required to more adequately understand the mechanisms underlying these observations and to determine the driving forces for this transformation.

Acknowledgements

The LLNL portion of this work was performed under the auspices of the U.S. Department of Energy, University of California Lawrence Livermore National Laboratory under contract W-7405-Eng-48. The ORNL portion of this research was sponsored by the U. S. Department of Energy, Division of Materials Science and Engineering, U. S. Department of Energy, under contract DE-AC05-00OR22725 with UT-Battelle, LLC.

References

1. J.W. Elmer, Joe Wong, M. Fröba, P.A. Waide, and E.M. Larson: *Metall. Mater. Trans. A*, 27A, 775-83 (1996)
2. J.W. Elmer, Joe Wong, and T. Ressler, *Metall. Mater. Trans. A*, 29A, 2761-2773 (1998)
3. T. Ressler, Joe Wong, and J.W. Elmer, *J. Phys. Chem. B*, 102, 10724-10735 (1998)
4. Z. Yang, J.W. Elmer, J. Wong, and T. DebRoy, *Weld J.*, 79(4), 97s–111s (2000)
5. J.W. Elmer, Joe Wong, and T. Ressler, *Metall. Mater. Trans. A*, 32A, 1175-1188 (2001)
6. J.W. Elmer, Joe Wong, and T. Ressler, *Scripta Mater.*, 43(8) 751-757 (2000)
7. J.W. Elmer, Joe Wong, and T. Ressler, in *Joining of Advanced Specialty Materials II*, p 200, ASM International, Materials Park, OH (2000)
8. S.S. Babu, J.W. Elmer, S.A. David, and M. Quintana, Proc. Roy Soc. A, in press (2002)
9. T.A. Palmer, J.W. Elmer, and J. Wong, *Sci. Technol. Weld. Join.*, in press (2002)
10. K. Mundra, T. DebRoy, and K.M. Kelkar, *Numer. Heat Trans. A*, 29, 115-129 (1996)
11. Z. Yang and T. DebRoy, *Metall. Mater. Trans. B*, 30B, 483-493 (1999)
12. Z. Yang, *Modeling Weldment Macro and Microstructure from Fundamentals of Transport Phenomena and Phase Transformation Theory*, Ph.D. Thesis, The Pennsylvania State University (2000)
13. W. Pitscheneder, T. DebRoy, K. Mundra, and R. Ebner, *Weld. J.*, 75(3), 71s-80s (1996)
14. H. Hemmer and Ø. Grong, *Metall. Mater. Trans. A*, 30A, 2915-29 (1999)
15. H. Hemmer, Ø. Grong, and S. Klokkehaug, *Metall. Mater. Trans. A*, 31A, 1035-48 (2000)
16. V. Karpenko, J.H. Kinney, S. Kulkarni, K. Neufeld, C. Poppe, K.G. Tirsell, J. Wong, J. Cerino, T. Troxel, J. Yang, E. Hoyer, M. Green, D. Humpries, S. Marks, and D. Plate, *Rev. Sci. Instrum.*, 60, 1451-1460 (1989)
17. *PowderCell, v. 1.0*, Federal Institute for Materials Research and Testing, Rudower Chaussee 5, 12489 Berlin, Germany
18. G.T. Eldis, *Metall. Soc. AIME*, 126-157 (1978)
19. J.M. Vitek, S.A. Vitek, and S.A. David, Metall. Mater. Trans. A, 26A, 2007-2025 (1995)
20. J.M. Vitek, E. Kozeschnik, and S.A. David, Calphad, 25(2), 217-230 (2001)
21. F.D. Fischer, F.G. Rammerstorfer, and F.J. Bauer, Metall. Trans. A, 21A, 935-948 (1990)
22. T. Siegmund, E. Werner, and F.D. Fischer, J. Mech. Phys. Solids, 43(4), 495-532 (1995)